An individual-based movement model for contacts between mule deer (*Odocoileus hemionus*)

Kelsey Gritter, Maria Dobbin, Evelyn Merrill & Mark A. Lewis

2024

Ecological Complexity 58 (2024) 101082

Contents lists available at ScienceDirect

Ecological Complexity

journal homepage: www.elsevier.com/locate/ecocom

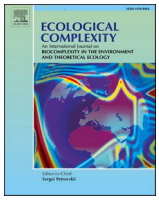

Original Research Article

An individual-based movement model for contacts between mule deer (*Odocoileus hemionus*)

Kelsey Gritter [a,b], Maria Dobbin [a], Evelyn Merrill [a], Mark Lewis [c,*]

[a] Department of Biological Sciences, University of Alberta, Canada
[b] Northern Forestry Centre, Canadian Forest Service, Natural Resources Canada, Edmonton, Alberta, Canada
[c] Department of Mathematical and Statistics, and Department of Biology, University of Victoria, Canada

ARTICLE INFO

Keywords:
Individual-based model
Within-group contacts
Between-group contacts
Contact rates
Mule deer
Step-selection function

ABSTRACT

Contacts between individuals are key for the spread of infectious disease. Although essential to understanding disease spread, contact rates are difficult to predict, based simply on population demographics in wildlife populations, because contact rates depend upon environmental features as well as the nature of social interactions within and between groups of individuals. We developed a detailed, behaviorally structured, individual-based model (IBM) in Netlogo to simulate contacts between- and within-groups of individual mule deer (*Odocoileus hemionus*), a species particularly susceptible to chronic wasting disease. The model tracks contacts (defined as two individuals coming within five meters of one another), recorded as between- or within-group depending on the social group membership of the two individuals (dyad). We parameterized the model with data from mule deer with global positioning systems (GPS) collars in east-central Alberta, Canada. Individuals move according to habitat preferences, home range attraction, and grouping behaviours. Animals were tracked at two-hour time steps and were modelled as selecting locations relative to preferred resources based on sex-specific integrated step-selection functions (iSSFs) with steps biased toward a home range centroid. Total within-group contacts increased with group size and were sensitive to changes in movement cohesion of the group and movement persistence, particularly movement cohesion. Total between-group contacts were sensitive only to the number of groups. We compared model predictions for where the locations of deer contacts occurred against an existing statistical model for the relative contact probabilities (RCP) on the same landscape (Dobbin et al. 2023). Predicted locations of deer contacts generally were consistent with higher predicted RCP values. When disease transmission is a function of contact rate, the model can be used to assess the interaction between model components (e.g., movement rates, grouping rules, home ranges, animal densities) and the spatial distribution of key natural and artificial resources that may attract deer and potentially increase disease spread.

1. Introduction

Disease can negatively affect populations and ecosystems by causing mortality directly or lowering individual fitness (McCallum et al., 2009; Cotterill et al. 2018). In turn, disease-driven declines in some species can alter ecosystem function (Herrera and Nunn 2019). A range of modelling tools from top-down, compartmental and ordinary differential equations models to bottom-up, individual-based models (IBMs) have been used to gain insight to address the impact of diseases on species and ecosystems (White et al. 2018a; Wells et al. 2019; Croft et al. 2020). Epidemiological studies using compartment models and ordinary differential equations can address questions related to pathogen invasion, disease dynamics and persistence, and population thresholds. However, because they employ population averages and do not let each individual have unique values and combinations of parameters (Murphy et al. 2020; Mortensen et al. 2021), they provide limited insight on the effect that small-scale, individual variation in host responses to heterogeneity in environmental conditions have on disease dynamics.

In contrast, bottom-up IBMs have the advantage of including spatial and, uniquely, individual heterogeneity, allowing for variation between individuals in behaviour and state variables (White et al. 2018a; Kerr 2019; An et al. 2020). For example, Scherer et al. (2020) found that predicted probabilities of disease persistence were up to eight times higher when the underlying habitat structure was accounted for in

* Corresponding author.
E-mail address: marklewis@uvic.ca (M. Lewis).

https://doi.org/10.1016/j.ecocom.2024.101082
Received 23 June 2023; Received in revised form 17 November 2023; Accepted 16 April 2024
Available online 27 April 2024

individual movement. Responses to environmental heterogeneity may be particularly important for wide-ranging hosts, such as large mammals, where the behavioral interactions with the environment, such as habitat selection while moving, can influence host interactions and alter disease spread (Scherer et al. 2020; Accolla et al. 2021). Further, IBMs can incorporate host grouping patterns and their correlated movements, which may influence rates of contacts and disease transmission (Schauber et al. 2007; Tosa et al. 2015; Belsare et al. 2020; Kjær and Schauber 2022). As a result, IBMs lend themselves to determining the sensitivity of model outcomes to changes in individual behaviors, and evaluating the impact of different environmental conditions on disease transmission (Ramsey et al. 2014; Kerr 2019; Maloney et al. 2020). This is particularly useful for evaluating disease management strategies that focus on altering host densities or the spatial pattern in resources influencing their movement and distribution. At the same time, IBMs require a large amount of data to parameterize and can be highly computationally expensive (Crooks et al. 2008; White et al. 2018a)

In this paper, we develop an IBM to simulate seasonal within- and between-group contacts of mule deer on a real, heterogeneous landscape and record contact rates by deer and by patch, to address the question of whether an IBM can be used to simulate realistic contact locations, and therefore provide a tool to evaluate management scenarios. The IBM incorporates resource selection in the location of the home range and in the movement steps of individuals, include interactions between individuals, and focus on winter behavior of deer, where group sizes are larger and the sex composition of groups is mixed (Lingle 2003). The model can be used to address applied questions such as how the density and spatial distribution of natural and artificial resources (e.g., food items) influence contact rates (Gritter 2022), the degree to which frequency- and density-dependent transmission influence disease dynamics (Manlove et al. 2017), and how different placement strategies of oral vaccine baits influence their rates of encounter (Thulke and Eisinger 2008; Ramsey and Efford 2010).

We start by giving an overview of all models and analyses, with the detailed presentation of the IBM simulation model details sequestered to Appendix A in a standard presentation format (Grimm et al. 2006, 2010, 2020). We perform a sensitivity analysis on model parameters (group cohesiveness, movement persistence, number of groups) to identify model output patterns in response to parameter changes, model robustness, and key parameters driving outputs (Cariboni et al. 2007; ten Broeke et al. 2016; Manlik et al. 2018; Prieto and Ibarguen-Mondragon 2019). Finally, we evaluate whether the model can produce realistic outcomes by comparing a map of the spatial distribution of simulated contacts across a real-world landscape to a map of the probability of contacts occurring in a location, which was derived statistically by Dobbin et al. (2023) based on known contacts of GPS-collared deer.

2. Methods

2.1. Animal data

We used data from GPS-collared mule deer in east-central Alberta, Canada (animal use protocols: Univ. Alberta 4641001 and AUP00001369). Two-hour fix data were used for the integrated step-selection functions, and data were rarefied to one fix per quarter of the day for the home range resource selection functions. The margin of error for the GPS collars across habitats and time periods ranged from 4.5 $\pm$ 0.2 m to 7.5 $\pm$ 0.2 m. Winter deer densities, group size, and composition of groups were based on winter aerial surveys during 2008, 2009, 2018, and 2020, whereas 81 GPS-collared mule deer, monitored over two periods (2006 - 2009, 2017 - 2020), provided the basis for home-range sizes, home-range resource selection function, and movement integrated step-selection functions.

2.2. Models and analysis

In this paper, there are multiple analyses used to create and evaluate the individual-based model. The relationship between these analyses can be seen below in Fig. 1.

2.2.1. Home-range resource selection functions

The model focuses on contact rates in winter when mule deer are more concentrated and form larger, mixed-sex groups (Lingle 2003). We assumed home-range sizes and habitat selection patterns remain constant throughout the simulation, but the model could be extended to include changes in behaviour within or across seasons.

Sex-specific resource selection functions (RSFs) were developed for home range placement, because the sexes have different median home-range sizes. These were based on empirical data from winter/spring (16 December – 9 May). The winter home-range selection function was derived using movement data from 54 female and 21 male GPS-collared mule deer, each of which had between 309 and 584 fixes (GPS locations) for the winter when including only one fix from each quarter day. Then home ranges were delineated base on 95 % utilization distributions calculated with the `adehabitatHR` (version 0.4.19) software package in R (Calenge, 2006). The analysis was based on a "used" versus "available" structure for the home range habitat. Home ranges (used units, denoted by 1) derived from the empirical data were compared to randomly placed circular areas (available units, denoted by 0), where available units were equal in area to the median home-range size (16.05 km^2 for males, 14.36 km^2 for females) and the entire landscape was assumed to be available. Median home-range size was used to represent the deer instead of the mean to avoid overrepresentation of large home-range values that resulted from dispersal movements included in the GPS data. Five available units were generated for each used unit (Gustine et al. 2006; Ladle et al. 2018).

Covariate values for each used and available home range unit (Table 1) were measured using the average covariate value within the home range. Distance covariates were transformed using a negative exponential function in order to represent a more realistic effect of these features. Transforming the distance values restricts the effect of features past a particular distance as opposed to allowing for continued effects of a feature at an unrealistic distance (Nielsen et al. 2009). Covariates were assessed for collinearity and variables correlated with $|r| > 0.7$ were not included in the same RSF model. RSF models were fit using a generalized linear model with a logistic function, with the dependent variable being whether the home range was used (1) or available (0) (Boyce et al. 2002; Bates et al. 2015). The `lme4` (version 1.1–26) package in R was used for a standard set of models plus the model including covariates that did not overlap zero in the global model. We initially fit home range RSFs separately for male and female mule deer to see if the top model was the same for both and to identify the set of candidate models for the mixed-sex analysis. However, there is an advantage to combining males and females if possible, because of the need to place mixed home-ranges with one home-range centroid for all group members (Lingle, 2003; unpublished data). Therefore, the top 5 models from males and females were taken as the candidate models for the winter category and male and female data were pooled to parameterize a winter RSF for both sexes (Appendix B). Spatial weights on the landscape were then calculated using home-range-sized moving window layers. Prior to creating mixed home-ranges, male and female RSF layers were calculated, as the sexes have different home-range sizes, and therefore a different moving window size was necessary. After the separate male and female layers were calculated a mixed RSF layer for both sexes was created by averaging the separate female and male layers with a 70:30 weighting for females: males.

We assessed the degree of support for each model of home-range selection based on Akaike's information criterion (AIC), corrected for small sample size, and parsimony. We assessed model performance using k-fold cross validation with a circular moving window to calculate

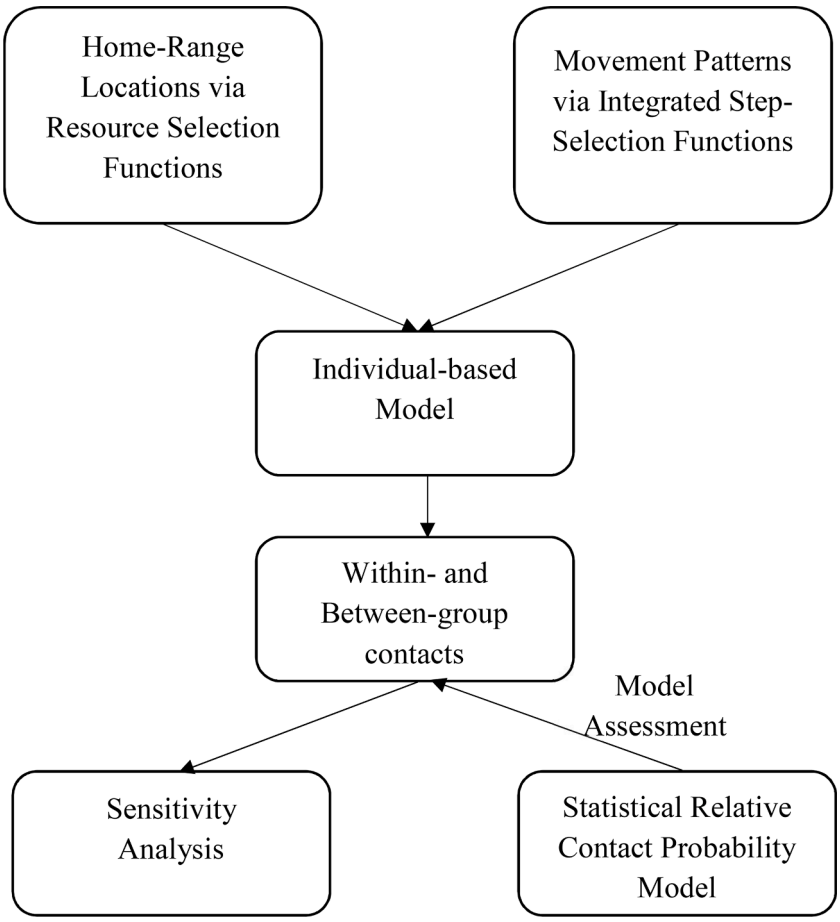

Fig. 1. Relationship between analyses used to create and evaluate the individual-based model presented in this paper.

covariate values for each cell (Burnham and Anderson 2002; Boyce et al. 2002).

2.2.2. Individual based model (IBM) for deer movement

The overall purpose of our individual-based model (IBM) was to realistically simulate within- and between-group contacts of mule deer on a real, heterogeneous landscape and to record contact rates by deer and by patch, and therefore provide a tool to evaluate management scenarios. Netlogo was used for programming the IBM as it is open source and relatively intuitive to program in.

Patterns that were expected to be reproduced include home range behaviours, within-group contacts being higher then between-group contacts, and habitat selection for more favourable environments. To consider our model sufficient for its purpose, realistic simulation of contacts was defined as congruence with empirical data on contacts collected via GPS-collared mule deer. The IBM incorporated key deer behaviours such as seasonal grouping, home ranges, and resource selection, with the aim of producing a depiction of potential contact rates and locations that may be representative of disease transmission on a heterogeneous landscape. State variables for the spatial patches and for the deer are given in Table 2. The spatial and temporal resolution and extent are given by Wildlife Management Unit (WMU) 234 in Alberta, Canada (UTM: xmin 528,756.4, xmax 566,706.4, ymin 5,816,805, ymax 5,854,755) over a winter-spring period (16 December – 9 May) broken into two-hour intervals.

The most important processes of the model, which are repeated every time step, are (i) calculation of turning angle distribution based on persistence and direction of home range centroid for all individuals, (ii) selection and movement of group leader and followers, and (iii) contacts, recorded by deer pair (hereafter referred to as dyad) and group type (see also Figure A.1).

The most important design concepts of the model are (i) emergence of patterns of space use (e.g., home-range size and shape), and of contacts between deer, (ii) sensing by deer of resource covariates, direction of home range centres and of leadership status, (iii) stochasticity with respect to home range placement and movement of deer, (iv) collective group formation by deer, and (v) observation of dyad-specific (FF, MM, MF) total within- and between-group contacts (recorded both by deer and by patch).

Details of the IBM simulation are given in Appendix A using the ODD protocol (Grimm et al., 2020).

2.2.3. Integrated step-selection function

A step-selection function (SSF) was used as a key ingredient for the IBM simulation for the movement of deer. Here we describe the Integrated Step-Selection Function (iSSF) method used to parameterize the movement weights for the SSF. We parameterized the iSSF weight by comparing covariate values associated with the end point of each step of a GPS-collared deer (used=1) to those at the end point of 15 random steps (used=0), initiated at the same location but with direction and step length chosen at random from the empirical distributions of the GPS-collared deer (Female = 52, Male = 25). We drew step lengths from an exponential distribution fit to data pooled across individuals for each sex and used a step-specific Von Mises modified turning angle distribution with empirically determined strength parameters $\kappa 1$ and $\kappa 2$ (details are given later in Equation 2). We measured the landscape attributes given in Table 1 at the end point of a step. Models were fit using a conditional logistic regression, using the `amt` (version 0.1) package in R (Signer et al. 2019). The candidate models included a set common to both sexes plus the model including only variables in the global model

Table 1
Variables, units, and analysis scale characterizing landscape attributes within 30-m patches in a landscape of east central Alberta, Canada used in simulating mule deer contact rates. All distance layers were transformed with a decay function: exp(−0.001*distance). A description of layer creation and visualization layers can be found in Gritter (2022).

Variable	Unit	Analysis scale	Description	Source
Distance to wells	m	–	Distance to nearest oil well site.	(Governement of Saskatchewan 2015; Alberta Energy Regulator 2020)
Distance to rivers	m	–	Rivers were all primary or secondary rivers in Alberta; in Saskatchewan rivers were the Battle River, North and South Saskatchewan River.	(Government of Canada 2017; Altalis 2018a)
Distance to streams	m	–	Streams included all permanent linear water feature besides Battle River, North Saskatchewan River, and South Saskatchewan River in Saskatchewan, and all perennial and indefinite streams in Alberta.	(Government of Canada 2017; Altalis 2018a).
Distance to roads	km	–	Distance to nearest road, paved and unpaved.	(Governement of Saskatchewan 2019; Altalis 2020).
Agriculture	%	250 m	Proportion agriculture land cover from Landsat imagery.	(Latifovic, 2019; Merrill unpublished data)
Woody cover	%	250 m	Proportion woody cover from TM Landsat imagery.	(Latifovic, 2019; Merrill unpublished data)
Woody cover edge	km/km^2	250 m	Linear density of woody cover edge.	(Latifovic, 2019; Merrill unpublished data)
Ruggedness	Unitless	30 m	Terrain ruggedness (Riley et al., 1999)	(Government of Canada 2016; Altalis 2018b).

that did not overlap zero for each sex. The top model for each sex/season was selected using AICc and parsimony.

2.2.4. Sensitivity analysis

We conducted a sensitivity analysis of three key model parameters while holding all other parameters constant. These three were chosen as they are the three variables with the most limited empirical data, whether from our studies or the literature, that could be used to inform their values. We varied the movement persistence parameter that influences home-range size (κ_1, see Equation 2, Appendix A), with values from 0 to 1. While holding population size constant we varied the number of groups from 196 to 240 to represent how aggregated deer were across the landscape as well as variation in group size. Finally, we varied the 30° restriction angle for the deer following the leader deer (described in Appendix A) to represent varying movement cohesion within deer herds. We employed a Latin hypercube sampling procedure using the `nlrx` (version 0.4) package in R (Salecker et al. 2019), using one hundred iterations, each running for 1840 timesteps. We present partial correlation coefficients (PCC) as well as partial rank correlation coefficients (PRCC) to look for non-linear effects (Helton and Davis 2003). Confidence intervals for the correlation coefficients were calculated using bootstrapping.

Table 2
State variables for patches and deer in the IBM.

Patches	
proportional-Mweight/ proportional-Fweight	Used to determine whether an individual accepts or rejects a step when simulating deer movement from the iSSF, calculated by dividing the cell weight (as determined by step-selection function) by the maximum weight across all cells
within-contacts-winter-XX / between-contacts-winter-XX	Total number of within/between-group contacts that have occurred on that cell between the given dyad type (female-female, FF MF; male-male, MM; male-female, MF).
Deer	
male?/female?	True/false variables that define the sex of the individual
Leader	True/false variable that defines the leader of the group
Group	Group number of the individual, defines group membership
Leaderangle	[who] (ID) of the deer in group with leader=true
HRX/HRY	x and y coordinates of the home range centre
Angle	The turning angle for the deer's step
step-length	The step length for the deer's step
Result	A 0/1 parameter, 0 when not accepting step, switches to 1 when step is accepted and breaks the loop in the code
Point	The proportional weight value of the cell to which the drawn step sends the individual
sine/cosine	Parameters calculated using the direction of persistence and direction towards the home range centre, used to determine the new heading for the individual
vm-length	Spread parameter for the Von mises turning angle distribution
Within-group-winter-same or mixed / between-group-winter-same or mixed	The total number of contacts that have occurred for that deer, with deer of the same sex and with deer of the opposite sex (mixed).
Step-within-winter-same or mixed /step-between-winter-same or mixed	The number of contacts occurring in the current step that are with the same sex or with the opposite sex (mixed).

2.2.5. Model assessment

We used predicted values from an empirically derived, statistical model of the relative probability of a contact (RCP) occurring at a location to assess the distribution of simulated contacts. RCP values for our study area were derived in Dobbin et al. (2023) where values represent the spatial probability of a direct contact (proximity $\leq$ 3 m) occurring between two mule deer collared in east-central Alberta (2019–2020). The RCP models were derived by comparing environmental characteristics (Table 1) at known contact locations (1) to those of random locations (0) within the space-use overlap of two GPS-collared mule deer using a logistic regression to derive the parameters of an exponential model. Contact probability can be dependent on environmental features as deer can avoid or select features that influence their movement and home-range selection. RCP values were scaled between 0 and 1 by dividing by the maximum value. High values indicate a high relative probability of deer contact at a location given its environmental characteristics (see Dobbin et al. 2023 for more details). Dobbin et al. (2023) used group- and dyad-type-specific RCP models to predict RCP values for each patch on the landscape. We compared these values to the number of contacts for a patch (Table 2) averaged from 10 simulations using ten different random seeds to determine where contacts were occurring. We used a two-tailed t-test to compare the mean RCP of cells where contacts occurred in the simulations to the mean RCP at the equivalent number of random points within the study area.

Random points were placed with an equal probability of placement across the landscape, with no two points in the same cell. Because the data were continuous and randomly sampled and had a sufficiently large sample size, the two distributions satisfied the requirements for performing a t-test.

3. Results

3.1. Home-range resource selection functions

There were 4 competing models (ΔAICc < 2) for the pooled mule deer selection of home range locations (see Section 2.2.1 for methods), and there was considerably more support for these models than the null model (Table 3). The top models all included distance to river, streams, well sites, and extent of woody cover, although models differed with respect to the linearity in the selection for woody cover. Deer avoided roads in 3 of the top models. We used the top, most parsimonious model, which reflected winter home ranges located in areas closer to large rivers and well sites, but further from streams and with more woody cover, with woody cover having the greatest influence on home range placement (Table 3).

RSF-selection values across the study area indicated that there was one large cluster of high RSF values in the center and one on the western portion of the study area, with a few other clusters scattered throughout that correspond to areas of high woody cover (Fig. 2). Five-fold cross validation revealed an average correlation of 0.82 ± 0.08 (± SD) between training and testing datasets for the winter RSF.

3.2. Integrated step-selection function

Empirical step length distributions of male and female deer (see Section 2.2.3 for methods) had exponential rate coefficients of −0.0037 and −0.0041, respectively (Fig. 3). Turning angle distributions were unique to every step of each individual due to the influence of persistence and bias to the home range centroid. The value of the κ_1 parameter, which influenced the persistence, and the κ_2, which influenced home range centroid bias using simulation were 0.4 and 0.5, respectively (Appendix C). When simulating, the same κ values and target home-range size were used for both sexes as their empirical median home-range size was less than one standard error different (target home-range size was 14.87 km^2, a 70:30 weighted average of female and male home-range sizes).

There were two competitive iSSF models (ΔAICc <2) for females and one iSSF model for males (Table 4). We used the model for females without the interaction between ruggedness and distance to the nearest river to simulate deer movements based on parsimony because including an interaction term did not considerably improve the model. Male iSSF models differed from that of females in that female step selection increased at high extents of woody cover whereas males selected high and low values of woody cover. In contrast, female movement was less influenced by the distance to well sites compared to males. Values of selection across the study area were generally high in the central-west and along the eastern edge of the study area. The distribution of step-selection values in the study area did not differ significantly between males and females (KS test D = 0.291, p < 0.001). While males and females select for similar areas, we do see some minor visual differences such as the males' higher selection values, especially in the center-west of the map, appear more diffuse than the females' values, likely because they also select for low woody cover values (Fig. 4).

3.3. Sensitivity

Partial correlation coefficients (PCC) revealed an extreme sensitivity of within-group contacts to movement cohesion (i.e., influencing proximity among individuals in a group), a slight sensitivity of within-group contacts to the number of groups, and a sensitivity of between-group contacts to the number of groups, while none of the other parameters have a substantial impact (all other confidence intervals overlap zero; Fig. 5a). PCC of movement cohesion was −0.93 for within-group contacts, indicating that as the restriction angle controlling movement cohesion increased and the group became less restricted in following the group leader, this resulted in fewer overall contacts within a group, but not between-group contacts. As the number of groups got larger, the number of between-group contacts and within-group contacts decreased as indicated by PCCs of −0.29 and −0.21, respectively. This is because we held the total number of individuals in the simulation constant, such that as the number of groups increased, number of individuals in a group (group size) decreased; therefore, there are fewer individuals contacting each other within groups, and in areas of overlap between groups there are now fewer individuals to contact each other resulting in fewer between-group contacts overall. Persistence, which influences home-range size, did not significantly affect within- or between-group contacts.

Partial rank correlation coefficients (PRCC) reveal non-linear influences not seen by looking at partial correlation coefficients (Fig. 5b). Within-group contacts remained extremely sensitive to movement cohesion (PRCC = -1.00), but were also sensitive to both number of groups (PRCC = -0.62) and movement persistence (PRCC = -0.29) in a non-linear manner. Between-group contacts were only slightly sensitive to the number of groups (PRCC = -0.26).

3.4. Model assessment

Mean RCP values at simulated contact locations were significantly higher than at random locations (Table 5), indicating that in all cases simulated contacts were more closely related to where real-world contacts are expected than would be at random except for where male-male, within-group contacts occur (Table 5, Fig. 6).

4. Discussion

We developed an IBM of mule deer to determine the spatial distribution of contact rates in heterogeneous landscapes. Although we parameterized the model for winter, the model could be extended to multiple seasons to incorporate changes in contact rates reflecting seasonal changes in movement rates, habitat selection, group composition and size, and home-range size. We assumed that within winter, home range location, group size, composition, and membership did not change. While previous IBMs for deer have included elements of home ranges and grouping, they have not incorporated habitat selection in

Table 3
Parameters of top models for the winter home-range resource selection function of mule deer based on pooled movement data of 54 female and 21 male GPS-collared mule deer in east-central Alberta, Canada. * indicates that the confidence interval does not overlap zero.

Intercept	Distance to rivers	Distance to roads	Rugged Terrain	Distance to streams	Woody cover	Woody cover^2	Distance to wells	ΔAICc
−4.64± 0.44*	**1.21± 0.36***			**−1.34± 0.65***	**7.48± 0.87***		**0.91± 0.31***	0
−5.59± 0.77*	0.97± 0.41*	−0.59± 0.58	0.91± 1.16	−1.33± 0.64*	16.94± 5.30*	−10.44± 5.70	1.09± 0.41*	0.462
−4.61± 0.44*	1.18± 0.36*	−0.60± 0.59		−1.30± 0.65*	7.46± 0.87*		1.17± 0.40*	0.962
−4.56± 0.45*	0.94± 0.41*	−0.63± 0.60	1.22± 1.16	−1.45± 0.65*	7.53± 0.88*		1.18± 0.41*	1.865
−419± 0.39*	0.85± 0.39*		1.28± 1.16	−1.21± 0.62*	6.91± 0.81*			6.953
−1.61±0.13*								128.16

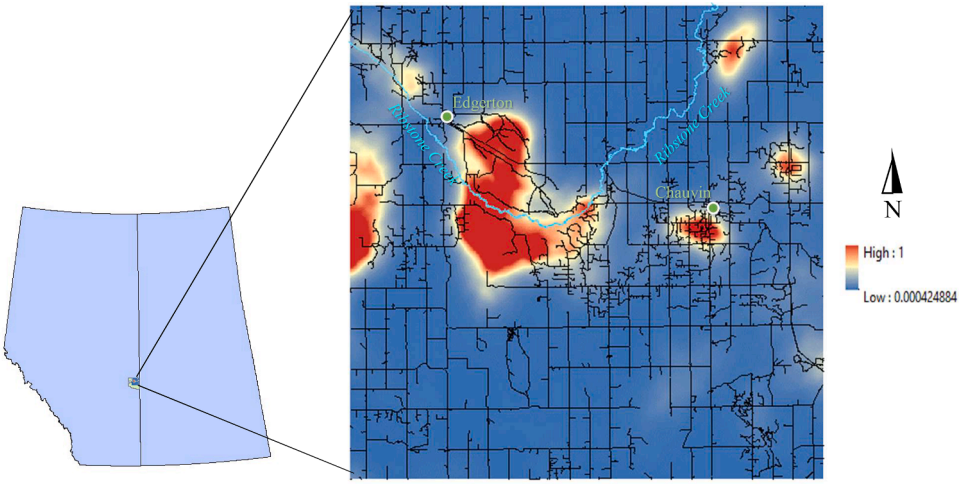

Fig. 2. Scaled, calculated winter home range RSF weights in simulation area based on weighted average of male and female calculated RSF layers. Green dots represent Edgerton (upper left) and Chauvin (center right).

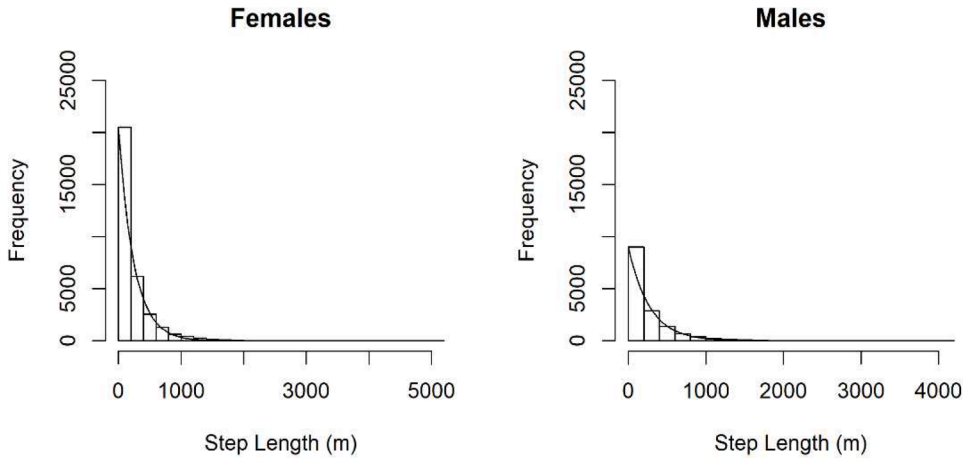

Fig. 3. Empirical step length distributions derived from mule deer movements in east-central Alberta, Canada using a two-hour fix rate and with exponential distribution fit lines overlaid.

Table 4
Parameter values for the top 3 sex-specific, integrated step-selection functions for mule deer in winter in east-central Alberta, Canada (F = 52, M = 25). Bolded is the top model, used to perform simulations, selected based on AICc and parsimony. * indicates that the confidence interval does not overlap zero.

	Agriculture	Edge density	Distance to rivers	Distance to roads	Rugg x Rivers	Rugged Terrain	Distance to streams	Woody cover	Woody cover^2	Distance to wells	ΔAICc
Male											
	−0.70± 0.09*	**0.09± 0.02***	**−0.10± 0.02***	**−0.16± 0.01***	**−0.11± 0.04***	**0.28± 0.02***	**−0.12± 0.02***	**−0.73± 0.26***	**0.73± 0.25***	**−0.03± 0.01***	0
	−0.69± 0.09*	0.09± 0.02*	−0.08± 0.02*	−0.16± 0.01*		0.28± 0.02*	−0.11± 0.02*	−0.70± 0.26*	0.70± 0.25*	−0.03± 0.01*	10.70
	−0.68± 0.09*	0.06± 0.01*	−0.08± 0.02*	−0.17± 0.01*		0.28± 0.02*	−0.12± 0.02*	0.03± 0.06		−0.03± 0.01	56.12
Female											
	−0.31± 0.06*	0.07 ± 0.008*	−0.05 ± 0.007*	−0.12 ± 0.009*	−0.02 ± 0.008*	0.25± 0.01*	−0.12± 0.01*	0.46± 0.04*			0
	−0.31± 0.06*	**0.07 ± 0.008***	**−0.05 ± 0.007***	**−0.12 ± 0.009***		**0.25± 0.01***	**−0.12± 0.01***	**0.46± 0.04***			1.87
	−0.31± 0.06*	0.06± 0.01*	−0.05 ± 0.007*	−0.12 ± 0.009*		0.25± 0.01*	−0.12± 0.01*	0.59± 0.17*	−0.13± 0.16	0.003± 0.007	5.01

home-range location and animal movement based on multiple environmental variables (Belsare et al. 2020; Mysterud et al. 2021; Kjær and Schauber 2022). However, in using an approach with habitat selection, we assumed deer had knowledge of surrounding habitats within its home range. Deer have been shown to have good memory when it comes to habitat, so it is not unrealistic that they would remember habitat within their home range, where they would typically be moving (Jakopak et al. 2019).

Our model corresponded well with statistical predictions of where the contacts were expected to occur based on a previous model (Dobbin

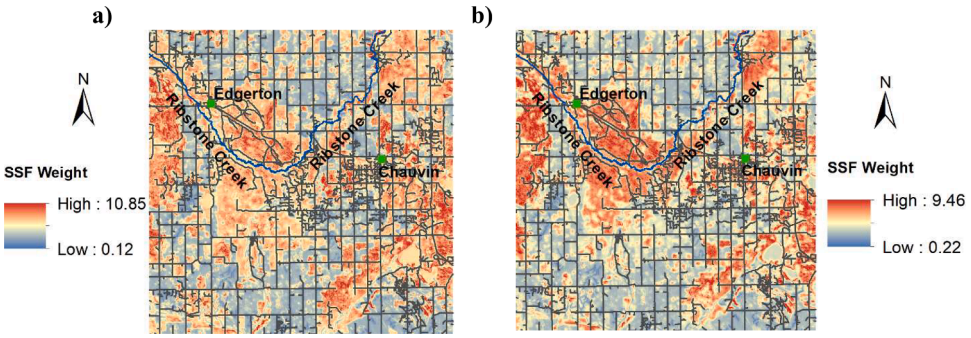

Fig. 4. Winter selection weights derived from empirical iSSF for a) male (n = 25) and b) female (n = 52) mule deer predicted for study area in east-central Alberta, Canada.

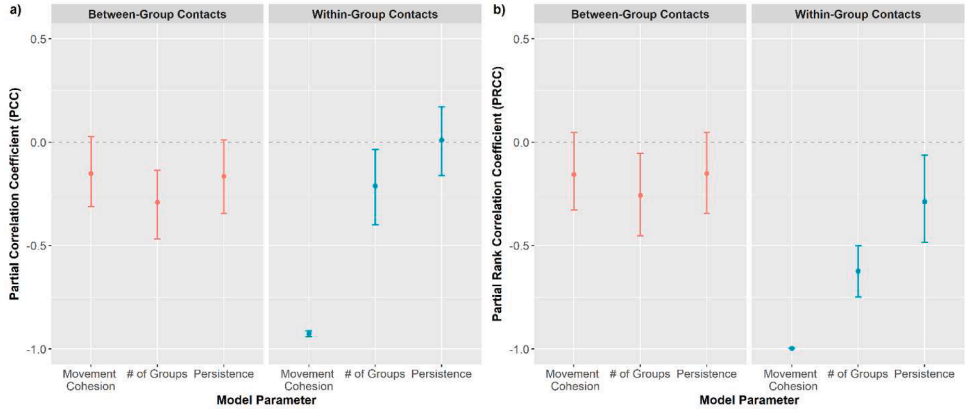

Fig. 5. Sensitivity plots for population between- and within-group contact metrics. For a), partial correlation coefficient is displayed on the y-axis, indicating sensitivity, whereas the test parameters of movement cohesion, number of groups, and movement persistence are on the x-axis. For b), partial rank correlation coefficient, looking for non-linear effects, is displayed on the y-axis, indicating sensitivity, whereas the test parameters of movement cohesion, number of groups, and movement are on the x-axis. Confidence intervals were obtained via bootstrapping.

Table 5
Mean (±SD) of relative contact probability (RCP, Dobbin et al. 2023) and t-test results comparing mean RCP values at locations where simulated contacts occurred and at random locations within the simulation landscape. Sample size (n) indicates the number of cells where contacts occurred and an equal number of random points.

	Mean RCP				
	Contact location	Random locations	t	p value	n
Within group					
Female-female	0.65 ± 0.05	0.59 ± 0.09	64.05	<0.001	13,823
Male-female	0.47 ± 0.07	0.35 ± 0.13	87.56	<0.001	10,852
Male-male	0.24 ± 0.05	0.25 ± 0.05	−0.21	0.835	2,578
Between groups					
Female-female	0.45 ± 0.04	0.40 ± 0.06	28.77	<0.001	2,002
Male-female	0.91 ± 0.04	0.69 ± 0.23	36.42	<0.001	1,564
Male-male	0.26 ± 0.06	0.24 ± 0.06	5.53	<0.001	379

et al. 2023). The RCP models and IBM use two different distance thresholds for a contact (3 vs. 5 m) and, therefore, do not represent the exact same measurement; however, we are simply using the RCP as a metric to assess the general areas where contacts are most likely to occur as predicted by the IBM. Indeed, because the contact locations emerging from the IBM have higher RCP values predicted from the statistical model than would be expected at random, we use this as support that our model reasonably predicts where contacts occur in space.

We attribute the correspondence in where contacts occurred in the study area between the IBM prediction and the empirically based, statistical model to several major components of the IBM. First, the initial locations of the deer in the simulation were informed by empirically based home-range selection patterns on the landscape. Indeed, in this landscape both males and females selected relatively similarly with woody cover being particularly important at both scales, which has been shown in previous studies (Habib et al., 2011; Nobert, 2012; VerCauteren and Hygnstrom, 2004). Second, similarity in what landscape features selected for in the iSSFs and RCPs contributed to the correspondence in outputs between the models. The majority of the variables, including agricultural areas, roads, ruggedness, woody cover, streams, and wells, were the same in both models. As a result, the environmental variables in the iSSF attract deer to specific types of areas within a home range, which can increase overlap at small scales leading to contacts occurring in those areas. Bonnell et al. (2010) also used an IBM for red colobus monkeys with resource selection influencing animal distribution. They showed that in an environment where there are few high-quality patches and individuals have a memory of those patches, use by multiple groups can increase between-group contacts and therefore facilitate disease transmission. Similarly, animals following the rules of the iSSF select for specific types of areas as they move across the landscape, which would draw individuals into high quality areas influencing where contacts are most likely to occur. High quality patches effectively increase local density and may facilitate more contacts between deer (Joly et al. 2006; Storm et al. 2013). In fact, White et al. (2018b), also using an IBM, found that strong resource selection and low resource availability in more fragmented landscapes promoted disease persistence and higher outbreak peaks (see also Kjær and Schauber

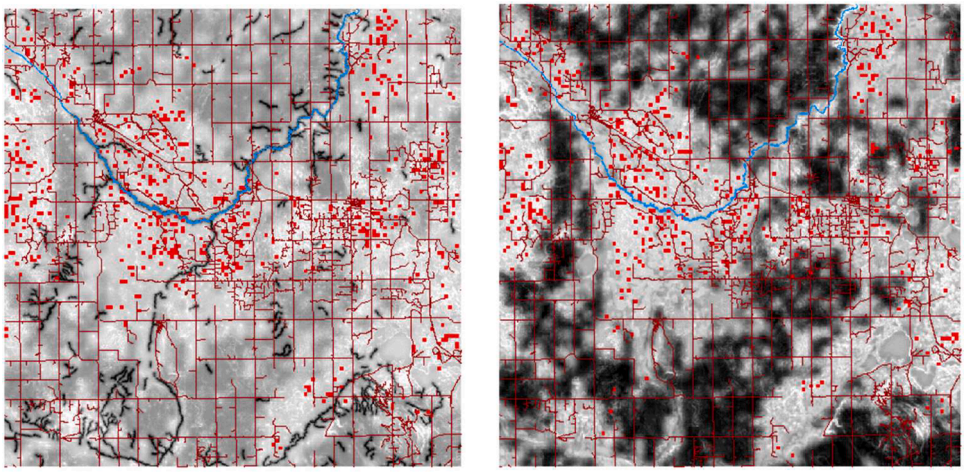

Fig. 6. Simulation contacts overlaid on relative contact probability layers (Dobbin et al. 2023) for within female-female (left) and within male-female (right). Simulation contacts were averaged across runs from 10 random seeds and resampled bilinearly to 300 m by 300 m from 30 m by 30 m for visibility. Red represents where contacts occurred in the simulation. Lighter indicates a higher value for the relative contact probability layers. Remaining overlays can be seen in Gritter (2022).

2022). This predicts that a more homogeneous landscape, where selected habitat is more evenly distributed, could help to reduce contacts as it would spread the deer out more over the landscape and not keep them all in the same few areas (Dion et al., 2011; Dion and Lambin, 2012; Habib et al., 2011; Real and Biek, 2007).

There were two discrepancies between the iSSFs and the RCP model in how environmental variables influenced where contacts occur. First, in both sexes individuals selected for areas of high edge density as they moved across the landscape, but the probability of a contact decreased in areas of high edge density. As edge densities increased, it is likely that the preference of deer for edges spread them out. Second, females selected for areas of high woody cover when moving across the landscape whereas high probabilities of contact reflected in RCP values were higher in areas of both low as well as high local woody cover. In low woody cover, this may not reflect the influence of preference but may reflect that deer group more tightly in open areas due to predation risk, increasing contacts (Lingle 2001; Lendrum et al. 2018). In high woody cover, individuals congregate in high quality areas, leading to more contacts.

Our model also predicted that contact rates within groups were higher than between groups, similar to what has been noted in field studies (Dobbin, 2022; Schauber et al., 2007). This was expected because we assumed cohesiveness in group movement and that the group stays together on the landscape. Overall, our average ratio of within:between-group contacts was ~ 6.98, which was low compared to those reported for real deer based on proximity of GPS-collared individuals or individuals with proximity loggers (from 5.0 to ~100; Dobbin, 2022; Schauber et al., 2007). Higher ratios of contacts among collared individuals within a group in the field, particularly with proximity collars, than we observed in our simulations, may reflect how collars record contacts and the density of groups in an area. We considered a contact to be when individuals are within 5 m of each other at 2-hr time step, whereas proximity collars reflect measurements made in continuous time. Thus, outputs of our IBM may not be comparable in terms of the magnitude of contact rates, but simulate where they are likely to occur.

At the same time, we provide insight on the sensitivities of within- and between-group contact rates to variation in model parameters. Contacts were sensitive to the number of groups and corresponding group size. The sensitivity of both within and between-group contacts to group size indicates that it is key to controlling contacts. Larger group size facilitates more contacts among individuals within a group as there are simply more individuals to come in contact with each other; at the same time it also influences between group contacts because there are potentially more individuals to contact each other in areas where the groups overlap (Cross et al. 2005b; White et al. 2017; Kjær and Schauber 2022). Unlike between-group contacts, within-group contacts also were sensitive to movement persistence, the variable which influences home-range size. As directional persistence, and therefore home-range size, increased, within-group contacts decreased, likely due to individuals being more spread out within their home range.

Within-group contact rate also was particularly sensitive to movement cohesion, as would be expected. Under high movement cohesion, individuals moved in a more unified direction, keeping them closer in proximity with others and more likely to contact each other. We did not include group fission-fusion dynamics, which would impact size of groups and within group contacts, and number of groups which could influence between group overlap and augment disease spread (Cross et al. 2005a; Aureli et al. 2012; Body et al. 2015). Including fission-fusion dynamics can be complicated because it is influenced by habitat, resources availability, group composition, and animal density (Raman 1997; Conradt and Roper 2000; Pays et al. 2012), although they could be key to looking at the networking between subgroups (Jepsen and Topping 2004; Ramos-Fernández et al. 2006). Belsare et al. (2020) included fission by having some members lose group membership if a group becomes too large, which is one possibility for how to incorporate fission in the future.

Although IBMs may not be able to address exact rates of contact in the real world, they can provide insight on the relative influence of different factors. For example, they could address questions such as how the density and arrangement of natural and artificial resources' (e.g., food items such as hay bales) influence potential contact rates (Gritter 2022), the degree to which frequency- and density-dependent transmission influence disease dynamics (Manlove et al. 2017), and how oral vaccine bait placement strategies influence the rates of encounter between animals (Ramsey and Efford, 2010; Thulke and Eisinger, 2008). Currently, the model outputs focus on contact rates as a surrogate for disease transmission. An extension of the IBM to disease dynamics could be to include the probability of disease transmission given a contact (Bonnell et al., 2010; White et al., 2018b). Including a constant transmission coefficient would allow for a simpler, less data intensive, population-average approach, while using a statistical distribution of different transmission coefficients, would allow for transmission heterogeneities due to contact duration and type of contact that depends on seasonal host behavior, within or between groups, such as aggression, reproductive or social attraction, or habitat-specific location, if data

were available (Dougherty et al. 2018). However, more behavioural detail would require a finer time step than the 2-hour timescale we used because of our movement data.

5. Conclusions

We found that incorporating social and habitat-based movement rules for individual mule deer in a heterogeneous environment produced within- and between- group patterns of contact rates consistent with the literature, and that our model predictions for contact locations corresponded with empirically derived locations of contact probability. Whereas between-group contacts were only sensitive to the number of groups/mean group size, within-group contacts also were sensitive to movement cohesion and movement persistence, reflecting the extent of areas over which deer travelled within their home ranges. Key extensions for our model to address disease spread would be to include heterogeneities in disease susceptibly of hosts and in transmission among individuals at locations, but this would require data on disease transmission and might require multiple time scales to model components like movement and duration of contact (Dougherty et al. 2018). Nevertheless, the current IBM can be applied to gain insight on a number of key questions focusing related to disease spread, such as the impact of landscape configurations and density of artificial attractants, as well as potentially informing any future vaccine programs. Our IBM also allows for the inclusion of key behaviours and heterogeneities to help produce insights on the factors most influencing outcomes, making them beneficial when evaluating environmental changes and management strategies.

CRediT authorship contribution statement

Kelsey Gritter: Conceptualization, Formal analysis, Methodology, Validation, Visualization, Writing – original draft, Writing – review & editing. **Maria Dobbin:** Conceptualization, Data curation, Writing – review & editing. **Evelyn Merrill:** Conceptualization, Data curation, Funding acquisition, Investigation, Methodology, Project administration, Resources, Supervision, Writing – original draft, Writing – review & editing. **Mark Lewis:** Conceptualization, Formal analysis, Funding acquisition, Investigation, Methodology, Project administration, Resources, Supervision, Writing – original draft, Writing – review & editing.

Declaration of competing interest

There are no conflicts of interest.

Data availability

Data will be made available on request.

Acknowledgements

We thank the Lewis Research Group and Merrill Lab for valuable discussion and feedback. Additionally, we thank the technicians who worked on the project including Johanna Thalmann, Gary Elaschuk, and Liam Horne. Finally, we thank two anonymous referees for helpful suggestions that greatly improved the manuscript.

Funding Sources

Evelyn Merrill gratefully acknowledges funding from the Government of Alberta, National Science and Engineering Research Council (NSERC; RGPIN-2016–04733), Rocky Mountain Elk Foundation (NA190034), Boone and Crockett, Wildlife Management Institute, Alberta Prion Research Institute, University of Alberta, Innovation Canada, Alberta Conservation Association (030–00–90–228), Northern Alberta Chapter of Safari Club International, and Alberta Fish and Game Association (MSL 2020 MD 04, MSL 2019 MD 03). Kelsey Gritter is grateful for support from the Government of Alberta, NSERC, and the University of Alberta. In addition, Mark Lewis gratefully acknowledges the Betty and Gilbert Chair in Mathematical Biology, the Canada Research Chair program and an NSERC Discovery grant (RGPIN-2018–05210).

Appendix A. Overview, Design concepts and Details (ODD) description of the Individual Based Model (IBM)

In this section we outline the IBM for the deer, based on the established ODD protocol (Grimm et al., 2020).

A.1. Overview

A.1.1. Purpose and Patterns

The purpose of this work is to use an IBM to simulate seasonal within- and between-group contacts of mule deer on a real, heterogeneous landscape and to record contact rates by deer and by patch, to address the question of if an IBM can be used to realistically simulate contacts, and therefore provide a tool to evaluate management scenarios. Realistic simulation of contacts will be defined as congruence with empirical data on contacts collected via GPS-collared mule deer. The IBM incorporates key deer behaviours such as seasonal grouping, home ranges, and resource selection, with the aim of producing a depiction of potential contact rates and locations that may be representative of disease transmission on a heterogeneous landscape. Patterns that are expected to be reproduced include home range behaviours, within-group contacts being higher then between-group contacts, and habitat selection for more favourable environments.

A.1.2. State Variables and Scales

Globals in the model include number of deer, number of HR centroids (determining the number of groups), total male and female weight (sum across all patches; Section 2.2.3), kappa-1 and kappa-2 (how much persistence versus the home range centre are favored in the direction of movement), and the turning angle restriction. The latter 3 variables are those required for home range behaviour and are explained further in section 2.5.3.1. There are two entities in the model, deer and patches, each with their own key set of state variables/variables (Table 2). The patches are characterized by the variable of input values representing landscape features, that remain constant, derived from GIS layers (Table 2), and state variables including proportional selection weights for the integrated step-selection functions, as well as outputs of cumulative between- and within-group contacts and cumulative contacts that have occurred on that patch by deer dyad type. Landscape covariates include vegetation features, topography, and distance to linear features, which are described in Table 1. Patches represent a 30-by-30-meter area for consistency across GIS layers representing environmental variables.

Individual deer variables include the movement variables necessary for an integrated step-selection function (iSSF; described in Section 2.2.3/ 2.5.3.2) including step length, turning angle, and the proportional weight at end point destination of the step. Each deer has its own turning angle distribution, a von Mises distribution, which depends on the vm-length that represents the agreement between the direction of persistence and the direction towards the home range centroid and impacts the spread of the von Mises distribution, as well as sine and cosine which are used to define the mean turning angle (see A3.3.1 for calculation details). Deer also have variables defining their ID (unique number for each deer), sex, group number, the ID of the group leader, and the x and y coordinates of their home range centre. Lastly, deer have variables defining their cumulative and step-specific number of contacts by group.

Timesteps representing two hours were used to run the simulation for a period representing winter-spring (16 December – 9 May, modified from Silbernagel et al. 2011, Dobbin et al. 2023) plus a 100-timestep burn-in period yielding 1840 timesteps. This temporal extent was chosen to limit the need for incorporating population dynamics such as reproduction and mortality; however, the model could be parameterized for other seasons. The total simulation area is 1440 km^2, which represents the largest square extent that can fit in the study area, with the study area being Wildlife Management Unit (WMU) 234, a portion of land in eastern Alberta.

A.1.3. Process Overview and Scheduling

Within each two-hour timestep, movement occurs in 3 stages in the order presented in Figure A.1. For each module, individuals and patches are processed in a random order.

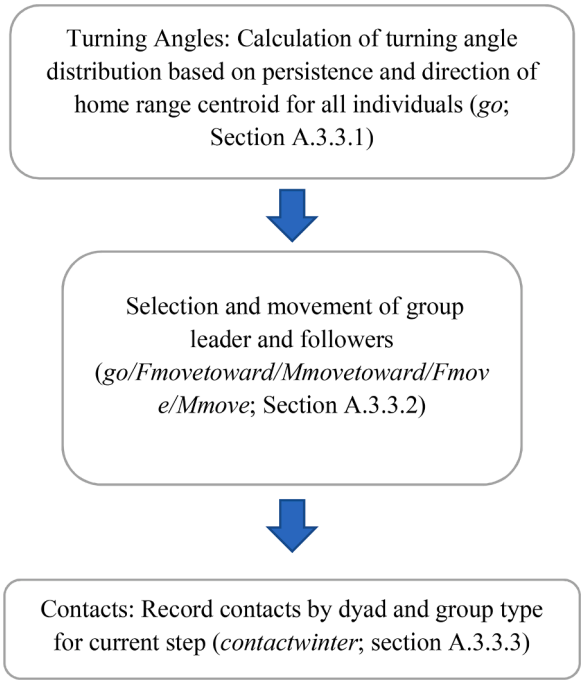

Fig. A.1. Flow chart depicting order of scheduling for the 3 major movement stages to recording contacts at each time step (italicized is the name(s) of the module(s) in the Netlogo code).

A.2. Design Concepts

A.2.1. Emergence

The contacts between deer are a focal output that emerges from the model, which are affected by the environment and submodels describing the deer's behaviour. Spatial use patterns are an emergent output that depends on the environmental input as well as the turning angle, and step length distributions. Home-range size and shape also are emergent outputs as they are the product of a step length distribution, a turning angle distribution modified for a bias to the home range centroid, habitat selection, and grouping behaviour.

A.2.2. Sensing

Deer are assumed to sense their environment, responding to resource covariates in the placement of their home ranges and their step-selection process. They are assumed to 'know' the resource covariates and the corresponding selection weight at the end point of every drawn step, which determines whether or not they accept the step (Fortin et al. 2005; Thurfjell et al. 2014). The deer also have an intuitive sense of the direction of their home range centre, incorporated as a bias towards their home range centre in calculating their turning angle parameters (Moorter et al. 2009; Duchesne et al. 2015). Deer within a group sense leadership status and consider it in their movements as the "followers" are required to move within a defined angle on either side of the direction of the group leader (Kjær and Schauber 2022).

A.2.3. Stochasticity

Stochasticity is included in the home range placement and movement of the deer. Deer are randomly placed on the landscape at the beginning of a simulation at one of the predetermined home-range centroids. Because each individual deer, rather than a group of deer, is located at a centroid, the exact group size and composition may vary slightly and differ with each iteration, although mean group size will stay the same because the number of groups correspond to the number of home range centroids. Stochasticity is also included in deer movement within a home range as steps are randomly

drawn from turning angle and step length distributions at every timestep. The sequential movement of deer proceeds via the acceptance-rejection method for each step (Appendix D), with the probability of a step being accepted proportional to the patch weight, adding stochasticity to the model (explained in section 2.3.3.3). We do not include stochasticity in resource weights of a patch.

A.2.4. Collectives

Deer form groups, corresponding to home range centroids, and exhibit grouping behaviour in their movement. Groups move using an approach of a leader moving and the other group members following the leader (Kjær and Schauber 2022). Groups will average ~6.6 individuals, which corresponds to a mixed-sex group in winter (Habib et al., 2011; Lingle, 2003; Merrill, Unpublished data). The model does not allow fission and fusion in group membership during an iteration.

A.2.5. Observation

The data collected from simulations for each deer and patch include the final value of the state variables of dyad-specific (MM, MF, or FF) total within- and between-group contacts (recorded both by deer and by patch). The state variables representing the number of contacts are cumulative throughout the simulation.

A.3. Details

A.3.1. Initialization

All model iterations were run in Netlogo with a sex ratio of 70:30 females to males and a density of 1 deer/km^2, which is within the ranges observed for mule deer in winter deer ground surveys in the study area (Merrill, unpublished data; Wilensky, 1999). Number of potential deer home ranges were determined by dividing deer population size by target group size (~6.6) and location of home range centroid was chosen based on a sex-specific, resource selection function derived from field data (see below). At the beginning of an iteration, each deer had a 0.7 probability of being female and 0.3 probability of being male. Deer were randomly placed at one of the potential home range centroids to create a mixed-sex group associated with each of the home range centroids, and group number was assigned based on centroid (group sizes ranged from 1 to 12).

A.3.2. Input

A.3.2.1. Home-range Placement. Home-range centroids were placed with the probability of a location being picked being proportional to the value of its resource selection function weight (Manly 2002; Lele et al. 2013). In ArcGIS, more than the required number of home ranges were placed on the landscape (1500), and then rarified to have the centroids be no less than 200 m apart (Comer et al., 2005; leaving 1092). Only 240 of these were used in the simulation and the subset was randomly selected from the 1092.

A.3.3. Submodels

At the beginning of each time step deer are moved to a new location in three stages (Fig. A.1).

A.3.3.1. Turning Angles. First, at each time step, a turning angle distribution for each individual (leader or follower) within each group is calculated. The turning angle distribution was derived based on the consensus method in Duchesne et al. (2015). Mean turning angle of the distribution (μ) was an angle between the direction of persistence (θ) and direction of home range (ψ) with the position being determined by κ values defining how much the deer favors persistence versus home range (Equation 1; Duchesne et al. 2015).

$$\mu = atan(\kappa_1 sin(\theta) + \kappa_2 sin(\psi), \kappa_1 cos(\theta) + \kappa_2 cos(\psi)). \tag{1A}$$

The spread of the turning angle distribution is defined by the agreement between the direction of persistence (θ) and direction of home range (ψ), defined by equation 2 (Fig. A.2).

$$\mathrm{K} = \sqrt{(\kappa_1 sin(\theta) + \kappa_2 sin(\psi))^2 + (\kappa_1 cos(\theta) + \kappa_2 cos(\psi))^2}. \tag{2A}$$

κ values for simulation were derived via simulation experiment and are not empirical (Appendix D).

A.3.3.2. Selection and movement of group leader and followers

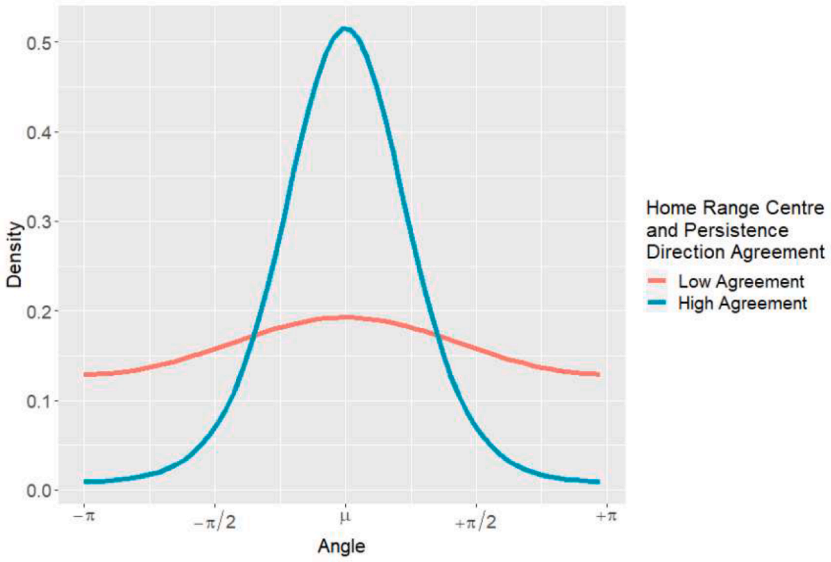

Fig. A.2. Graph of two von Mises distributions with two different levels of agreement between home range direction and persistence direction. Higher agreement between these directions results in a curve will less spread, while lower agreement results in a curve with more spread.

The leader of the group was the first individual to move at each time step and moved independently of every other individual in the group. A new group leader was randomly chosen with equal probability and designated as the leader, whose movement influences all other individuals in the group. This assumed both male and female deer could lead the group. The leader moved according to an integrated step-selection function (iSSF, Avgar et al., 2016), where the step length and turning angle are randomly chosen from their respective sex-specific distributions to move the leader to a new location. These locations are not restricted to patch centroids as the deer moved in the continuous space underlying the patches that represent environmental data. The sex-specific, exponential step length distribution was derived from empirical 2-hour GPS data pooled from GPS-collared mule deer whose movements were monitored in 2006–2009 (M = 11, F = 20) and 2017–2020 (M = 16, F = 34) in eastern Alberta (Merrill, unpublished data). Data used to parameterize the step length distribution were restricted to be above 20 m to avoid including spurious turning angles due to GPS error (Hurford 2009). However, when simulating movements, deer could select below 20 m because GPS error is not a concern when simulating movements. Turning angle was randomly chosen from the distribution of turning angles calculated for the individual animal as described above.

Once the leader selected a location, the location was either accepted or rejected by comparing the proportional weight of selection of the patch associated with the point at the end of the step to a random number between 0 and 1 (von Neumann, 1951; Appendix C). If that number was above the proportional weight, the step was rejected, and a new step was taken by redrawing from the step length and turning angle distribution until the step was accepted. Steps also were rejected if the target patch was occupied by more than 7 deer, corresponding to the average group size of 6.6, and two groups were constrained in occupying the patch at the same time. For groups of fewer than 7 deer it is possible that a deer from another group could land on the same patch and occupy the same area temporarily, but group composition would remain the same. Once the leader moved, other group members followed the leader but were required to select an angle that made them move within a restriction angle of 30° on either side of the leader (Belsare et al. 2020; Kjær and Schauber 2022). Proportional weights of rejecting and accepting a step were derived based on sex-specific iSSF (Avgar et al. 2016).

A.3.3.3. Contacts. A contact was defined for a current step when two deer came within 5 m of each other. We used 5 m to be approximate with contacts of 3 m that were used in the development of the statistical RCP model used for IBM assessment (Dobbin et al. 2023). The contact was classified as a between-group contact if the group number of the two individuals was different and otherwise as a within-group contact. At every time step, we recorded the number of conspecifics of each sex within 5 m. We summarized the total, cumulative winter contacts by group type (within or between) and by dyad type (female-female, FF; male-male, MM; female-male, MF) for each individual deer and for each patch in the landscape where a contact occurred. We counted contacts only after 100 timesteps to allow for a burn-in period that allowed the individuals to spread out and take a more natural positioning on the landscape.

Appendix B. Top 5 sex-specific winter resource selection functions

Table B.1.

Table B.1
Covariates included in the top 5 winter home-range resource selection functions for male and female mule deer.

	Distance to rivers	Distance to roads	Rugged Terrain	Distance to streams	Woody cover	Woody cover^2	Distance to wells
Males	✓	x	✓	✓	✓	x	x
	✓	✓	✓	✓	✓	x	x
	✓	x	x	✓	✓	x	✓
	✓	✓	✓	✓	✓	x	✓
	✓	✓	x	✓	✓	x	✓
Females	✓	✓	✓	✓	✓	✓	✓
	✓	x	x	✓	✓	x	✓

(*continued on next page*)

Table B.1 (*continued*)

Distance to rivers	Distance to roads	Rugged Terrain	Distance to streams	Woody cover	Woody cover^2	Distance to wells
x	x	x	x	✓	✓	x
✓	✓	x	✓	✓	x	✓
✓	✓	✓	✓	✓	x	✓

Appendix C. Home-range Size Simulation Testing

An experiment was done to determine the relative effect of kappa-1 and kappa-2 on home-range size, and which combination gives us the closest to our target home-range size of 14.87 km^2, which is based on the median 95% UD area for the winter-spring season. A simulation was run with 6 random seeds and uniform SSF weights, that went through kappa values from 0 to 1 by 0.1 and recorded the distance to home range centre for one of the seven individuals in the group at each timesteps. The 95% quantile was then taken and used to calculate home-range size for a given kappa-1, kappa-2 combination. This revealed that the larger the kappa-1: kappa-2 ratio was, the larger the HR size was. This makes sense as kappa-1 controls persistence while kappa-2 control bias towards the HR. In addition to this ratio being important, kappa-2 appears to have an impact on the standard deviation around a point. Therefore, a combination of kappa-1 = 0.4 and kappa-2 = 0.5 was chosen as this combination produced an average HR size of 14.64km^2 with a standard deviation of 2.38km^2. This was the best combination of proximity to the target HR size and low standard deviation.

Fig. C.1.

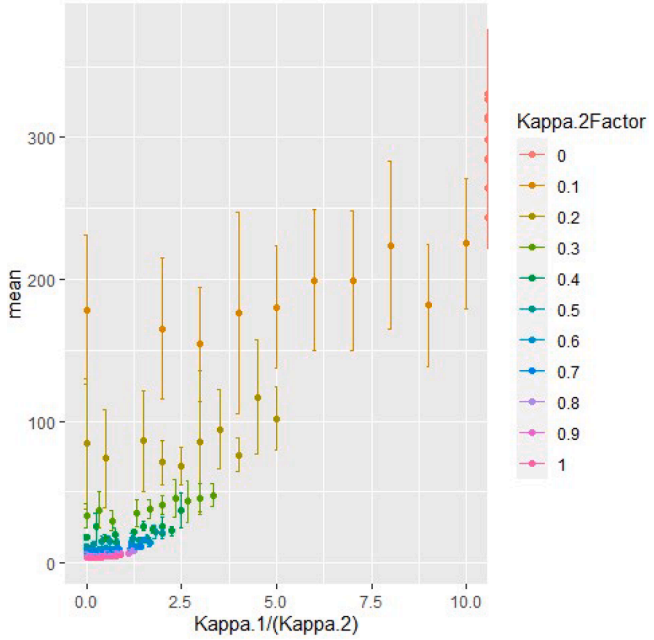

Fig. C.1. mean 95% utilization distribution home-range size (km^2) as a function of kappa-1 to kappa-2 ratio obtained from simulation with 6 different random seed for each combination. Kappa-1 and kappa-2 were varied from 0 to 1 by 0.1, but were never equal.

Appendix D. Step-selection function acceptance-rejection method theory

D.1. Step-Selection Function Background

The step-selection function is a probability density function based on current and previous locations, as well as environmental weightings:

$$f(x_{t+1}|x_t, x_{t-1}, Z(x_{t+1}), \psi) \tag{1D}$$

In this equation, $x_t \in \Omega \subset \mathbb{R}^2$ represents the position of the animal at time t, where Ω is the finite spatial domain of the animal, and $Z(x) : \Omega \to \mathbb{R}^m$ represents the environmental covariates where m is the number of covariates in the model. The vector $\psi \in \mathbb{R}^{m+2}$ represents the parameters in the model where $\psi = (\beta, \alpha, \kappa)$ has components $\beta \in \mathbb{R}^m$ describing covariate weights and $\alpha, \kappa \in \mathbb{R}$ describing step length and turning angle.

The probability density function can be represented by:

$$f(x_{t+1}|x_t, x_{t-1}, Z(x_{t+1}), \psi) = \frac{K(x_{t+1}|x_t, x_{t-1}, \kappa, \alpha) w(Z(x_{t+1})|\beta)}{\int_\Omega K(\xi|x_t, x_{t-1}, \kappa, \alpha) w(Z(\xi)|\beta) d\xi}. \tag{2D}$$

The weighting function $w : \mathbb{R}^m \to \mathbb{R}^+$ describes habitat selection preferences and the numerator represents the location at which a step finishes, x_{t+1}, in terms of the dispersal kernel K, and the weighting function w. The dispersal kernel itself depends on the locations at the previous two time steps, x_t and x_{t-1}, as well as the step length and turning angle parameters α *and* κ. The denominator ensures that function f is a probability density function, which integrates to 1. The dispersal kernel can be further broken down into a distribution for step length ζ, given by

$$K_1(\zeta|\alpha) \tag{3D}$$

and a distribution for turning angles, ψ, given by

$$K_2(\psi|\kappa). \tag{4D}$$

Here the step length is defined by

$$\zeta_t = |x_{t+1} - x_t| \tag{5D}$$

and the turning angle is defined as

$$\psi_t = \theta_t - \theta_{t-1} \tag{6D}$$

the increment in the bearing where, with $\Delta x_{2t} = x_{2t} - x_{2t-1}$ and $\Delta x_{1t} = x_{1t} - x_{1t-1}$:

$$\theta_t = \tan^{-1}\left(\frac{\Delta x_{2t}}{\Delta x_{1t}}\right) + \pi I(\Delta x_1 < 0) \tag{7D}$$

and the components of x_t are given by $x_t = \begin{pmatrix} x_{1t} \\ x_{2t} \end{pmatrix}$ where $I(\Delta x_1 < 0)$ represents the indicator function and is necessary to produce a range spanning the full unit circle due to the symmetry of arctan. Equations 5 to 7 yield the dispersal kernel as

$$K(x_{t+1}|x_t, x_{t-1}, \kappa, \alpha) = K_1(\zeta_{t+1}|\alpha)K_2(\psi_{t+1}|\kappa) \tag{8D}$$

where ζ_{t+1} is given in terms of x_{t+1}, x_t by equation 5 and ψ_{t+1} is given in terms of x_{t+1}, x_t, x_{t-1}, and κ by equations 6 and 7.

D.2. Acceptance-Rejection Method (von Neumann 1951)

This method simulates via an iterative process of randomly drawing steps until one that is accepted is found and then taking this step. Generating a value for simulation from a probability density function (pdf; f) via the rejection-acceptance method requires identifying a pdf, g, that is similar to one being simulated, but not identical, and that the ratio $\frac{f}{g}$ is bounded below a constant. When simulating an SSF, the dispersal kernel K(x) is taken to be the denominator distribution g, while the SSF is the distribution we are simulating from, f. This gives us

$$\frac{f(x)}{K(x)} = \frac{w(x)}{\int_\Omega K(\xi)w(\xi)d\xi} < c. \tag{9D}$$

Rearranged this gives us

$$\frac{f(x)}{K(x)} = \frac{w(x)}{c\int_\Omega K(\xi)w(\xi)d\xi} < 1. \tag{10D}$$

It is then easily seen that the numerator that will always make this true is when the maximum value of w in Ω is used as the denominator constant. For a perspective location, y, one then evaluates equation 11

$$p(y) = \frac{w(y)}{\underset{\xi\in\Omega}{max}(w(\xi))} \tag{11D}$$

generates a random value, u, from uniform(0,1), and then compares the two values. If u is less than p(y), then the step is accepted and the individual moves, if not, choose another step and repeat until a step is accepted.

References

Accolla, C., Vaugeois, M., Grimm, V., Moore, A.P., Rueda-Cediel, P., Schmolke, A., Forbes, V.E., 2021. A review of key features and their implementation in unstructured, structured, and agent-based population models for ecological risk assessment. Integr. Environ. Assess. Manage 17, 521–540.

Alberta Energy Regulator. 2020, July. ST37: List of Wells in Alberta. Alberta Energy Regulator.

Altalis. 2018a, March 5. Hydrography. Altalis.

Altalis. 2018b, April 20. 25m Raster DEM. Altalis.

Altalis. 2020, April 15. Access. Altalis.

An, L., Grimm, V., Turner II., B.L., 2020. Editorial: meeting grand challenges in agent-based models. J. Artif. Societies Social Simulation 23, 13.

Aureli, F., Schaffner, C.M., Asensio, N., Lusseau, D., 2012. What is a subgroup? How socioecological factors influence interindividual distance. Behavioral Ecol. 23, 1308–1315.

Avgar, T., Potts, J.R., Lewis, M.A., Boyce, M.S., 2016. Integrated step selection analysis: bridging the gap between resource selection and animal movement. Methods Ecol. Evol. 7, 619–630.

Bates, D., Bolker, B., Maechler, M., Walker, S., 2015. Fitting linear mixed-effects models using lme4. J. Stat. Softw. 67, 1–48.

Belsare, A.V., Gompper, M.E., Keller, B., Sumners, J., Hansen, L., Millspaugh, J.J., 2020. An agent-based framework for improving wildlife disease surveillance: a case study of chronic wasting disease in Missouri white-tailed deer. Ecol. Modell. 417, 108919.

Body, G., Weladji, R.B., Holand, Ø., Nieminen, M., 2015. Fission-fusion group dynamics in reindeer reveal an increase of cohesiveness at the beginning of the peak rut. Acta Ethol. 18, 101–110.

Bonnell, T.R., Sengupta, R.R., Chapman, C.A., Goldberg, T.L., 2010. An agent-based model of red colobus resources and disease dynamics implicates key resource sites as hot spots of disease transmission. Ecol. Modell. 221, 2491–2500.

Boyce, M.S., Vernier, P.R., Nielsen, S.E., Schmiegelow, F.K.A., 2002. Evaluating resource selection functions. Ecol. Modell. 157, 281–300.

Burnham, K.P., Anderson, D.R., 2002. Model Selection and Multimodel inference: a Practical Information-Theoretic approach. Pages 49–97 Model Selection and Multimodel Inference: A Practical Information-Theoretic Approach. Springer, New York, NY.

Calenge, C., 2006. The package adehabitat for the R software: tool for the analysis of space and habitat use by animals. Ecol. Modell. 197, 1035.

Cariboni, J., Gatelli, D., Liska, R., Saltelli, A., 2007. The role of sensitivity analysis in ecological modelling. Ecol. Modell. 203, 167–182.

Comer, C.E., Kilgo, J.C., D'Angelo, G.J., Glenn, T.C., Miller, K.V., 2005. Fine-scale genetic structure and social organization in female white-tailed deer. J. Wildlife Manage. 69, 332–344.

Conradt, L., Roper, T.J., 2000. Activity synchrony and social cohesion: a fission-fusion model Proceedings of the Royal Society of London. Series B: Biol. Sci. 267, 2213–2218.
Cotterill, G.G., Cross, P.C., Middleton, A.D., Rogerson, J.D., Scurlock, B.M., du Toit, J.T., 2018. Hidden cost of disease in a free-ranging ungulate: brucellosis reduces mid-winter pregnancy in elk. Ecol. Evol. 8, 10733–10742.
Croft, S., Massei, G., Smith, G.C., Fouracre, D., Aegerter, J.N., 2020. Modelling spatial and temporal patterns of African swine fever in an isolated wild boar population to support decision-making. Front. Vet. Sci. 7.
Crooks, A., Castle, C., Batty, M., 2008. Key challenges in agent-based modelling for geo-spatial simulation. Comput. Environ. Urban. Syst. 32, 417–430.
Cross, P.C., Lloyd-Smith, J.O., Getz, W.M., 2005a. Disentangling association patterns in fission–fusion societies using African buffalo as an example. Anim. Behav. 69, 499–506.
Cross, P.C., Lloyd-Smith, J.O., Johnson, P.L.F., Getz, W.M., 2005b. Duelling timescales of host movement and disease recovery determine invasion of disease in structured populations. Ecol. Lett. 8, 587–595.
Dion, E., Lambin, E.F., 2012. Scenarios of transmission risk of foot-and-mouth with climatic, social and landscape changes in southern Africa. Appl. Geography 35, 32–42.
Dion, E., VanSchalkwyk, L., Lambin, E., 2011. The landscape epidemiology of foot-and-mouth disease in South Africa: a spatially explicit multi-agent simulation. Ecol. Modell. 222, 2059–2072.
Dobbin, M., 2022. Masters Thesis Analysis of Direct Contacts Between Mule Deer (*Odocoileus hemionus*). University of Alberta.
Dobbin, M.A., Smolko, P., Put, L., Merrill, E.H., 2023. Risky business: relating probability of direct contact to risk of chronic wasting disease. Front. Ecol. Evol. 11.
Dougherty, E.R., Seidel, D.P., Carlson, C.J., Spiegel, O., Getz, W.M., 2018. April. Going Through the Motions: Incorporating Movement Analyses into Disease Research. Blackwell Publishing Ltd.
Duchesne, T., Fortin, D., Rivest, L.P., 2015. Equivalence between step selection functions and biased correlated random walks for statistical inference on animal movement. PLoS. One 10, e0122947.
Fortin, D., Beyer, H., Boyce, M., Smith, D., Duchesne, T., Mao, J., 2005. Wolves influence elk movements: behavior shapes a trophic cascade in Yellowstone National Park. Ecology 86, 1320–1330.
Governement of Saskatchewan, 2015. November 18. Vertical Wells. Government of Saskatchewan.
Governement of Saskatchewan, 2019. February. Saskatchewan Upgraded Road Network. Government of Saskatchewan.
Government of Canada, 2016. Canada Digital Elevation Model. October 21. Government of Canada.
Government of Canada, 2017. Lakes and Rivers in Canada - Canvec – Hydro Features. December 15. Government of Canada.
Grimm, V., Berger, U., Bastiansen, F., Eliassen, S., Ginot, V., Giske, J., Goss-Custard, J., Grand, T., Heinz, S.K., Huse, G., Huth, A., Jepsen, J.U., Jørgensen, C., Mooij, W.M., Müller, B., Pe'er, G., Piou, C., Railsback, S.F., Robbins, A.M., Robbins, M.M., Rossmanith, E., Rüger, N., Strand, E., Souissi, S., Stillman, R.A., Vabø, R., Visser, U., DeAngelis, D.L., 2006. A standard protocol for describing individual-based and agent-based models. Ecol. Modell. 198, 115–126.
Grimm, V., Berger, U., DeAngelis, D.L., Polhill, J.G., Giske, J., Railsback, S.F., 2010. The ODD protocol: a review and first update. Ecol. Modell. 221, 2760–2768.
Grimm, V., Railsback, S.F., Vincenot, C.E., Berger, U., Gallagher, C., DeAngelis, D.L., Edmonds, B., Ge, J., Giske, J., Groeneveld, J., Johnston, A.S.A., Milles, A., Nabe-Nielsen, J., Polhill, J.G., Radchuk, V., Rohwäder, M.-S., Stillman, R.A., Thiele, J.C., Ayllón, D., 2020. The ODD protocol for describing agent-based and other simulation models: a second update to improve clarity, replication, and structural realism. J. Artif. Societies Social Simulation 23, 7.
Gritter, K., 2022. Individual-based Movement Model of Mule Deer (*Odocoileus hemionus*) Contacts and Application to Artificial Attractants. University of Alberta, Edmonton, Alberta.
Gustine, D.D., Parker, K.L., Lay, R.J., Gillingham, M.P., Heard, D.C., 2006. Interpreting resource selection at different scales for woodland caribou in winter. J. Wildlife Manage. 70, 1601–1614.
Habib, T., Merrill, E., Pybus, M.J., Coltman, D., 2011. Modelling landscape effects on density–contact rate relationships of deer in eastern Alberta: implications for chronic wasting disease. Ecol. Modell. 222, 2722–2732.
Helton, J.C., Davis, F.J., 2003. Latin hypercube sampling and the propagation of uncertainty in analyses of complex systems. Reliab. Eng. Syst. Saf. 81, 23–69.
Herrera, J., Nunn, C.L., 2019. Behavioural ecology and infectious disease: implications for conservation of biodiversity. Philosophical transactions. Prog. Nucl. Energy 6. Biol. Sci. 374, 20180054.
Hurford, A., 2009. GPS measurement error gives rise to spurious 180° turning angles and strong directional biases in animal movement data. PLoS. One 4, e5632.
Jakopak, R.P., Lasharr, T.N., Dwinnell, S.P.H., Fralick, G.L., L.Monteith, K., 2019. Rapid acquisition of memory in a complex landscape by a mule deer. Ecology 100, 1–4.
Jepsen, J.U., Topping, C.J., 2004. Modelling roe deer (*Capreolus capreolus*) in a gradient of forest fragmentation: behavioural plasticity and choice of cover. Can. J. Zool. 82, 1528–1541.
Joly, D.O., Samuel, M.D., Langenberg, J.A., Blanchong, J.A., Batha, C.A., Rolley, R.E., Keane, D.P., Ribic, C.A., 2006. Spatial epidemiology of chronic wasting disease in Wisconsin white-tailed deer. J. Wildl. Dis. 42, 578–588.
Kerr, C.C. 2019. Is epidemiology ready for big software? pathogens and disease 77.
Kjær, L.J., Schauber, E.M., 2022. The effect of landscape, transmission mode and social behavior on disease transmission: simulating the transmission of chronic wasting disease in white-tailed deer (*Odocoileus virginianus*) populations using a spatially explicit agent-based model. Ecol. Modell. 472, 110114.
Ladle, A., Galpern, P., Doyle-Baker, P., 2018. Measuring the use of green space with urban resource selection functions: an application using smartphone GPS locations. Landsc. Urban. Plan. 179, 107–115.
Latifovic, R., 2019. November 1. 2015 Land Cover of Canada. Government of Canada; Natural Resources Canada; Canada Centre for Remote Sensing.
Lele, S.R., Merrill, E.H., Keim, J., Boyce, M.S., 2013. Selection, use, choice and occupancy: clarifying concepts in resource selection studies. J. Animal Ecol. 82, 1183–1191.
Lendrum, P.E., Northrup, J.M., Anderson, C.R., Liston, G.E., Aldridge, C.L., Crooks, K.R., Wittemyer, G., 2018. Predation risk across a dynamic landscape: effects of anthropogenic land use, natural landscape features, and prey distribution. Landsc. Ecol. 33, 157–170.
Lingle, S., 2001. Anti-predator strategies and grouping patterns in white-tailed deer and mule deer. Ethology 107, 295–314.
Lingle, S., 2003. Group composition and cohesion in sympatric white-tailed deer and mule deer. Can. J. Zool. 81, 1119–1130.
Maloney, M., Merkle, J.A., Aadland, D., Peck, D., Horan, R.D., Monteith, K.L., Winslow, T., Logan, J., Finnoff, D., Sims, C., Schumaker, B., 2020. Chronic wasting disease undermines efforts to control the spread of brucellosis in the Greater Yellowstone Ecosystem. Ecol. Appl. 30, e02129.
Manlik, O., Lacy, R.C., Sherwin, W.B., 2018. Applicability and limitations of sensitivity analyses for wildlife management. J. Appl. Ecol. 55, 1430–1440.
Manlove, K.R., Cassirer, E.F., Plowright, R.K., Cross, P.C., Hudson, P.J., 2017. Contact and contagion: probability of transmission given contact varies with demographic state in bighorn sheep. J. Animal Ecol. 86, 908–920.
Manly, B.F.J., 2002. Resource Selection By animals : Statistical Design and Analysis for Field Studies, 2nd ed. Kluwer Academic Publishers.
McCallum, H., Jones, M., Hawkins, C., Hamede, R., Lachish, S., Sinn, D.L., Beeton, N., Lazenby, B., 2009. Transmission dynamics of Tasmanian devil facial tumor disease may lead to disease-induced extinction. Ecology 90, 3379–3392.
Moorter, B., Visscher, D., Benhamou, S., Börger, L., Boyce, M., Gaillard, J.M., 2009. Memory keeps you at home: a mechanistic model for home range emergence. Oikos 118, 641–652.
Mortensen, L.O., Chudzinska, M.E., Slabbekoorn, H., Thomsen, F., 2021. Agent-based models to investigate sound impact on marine animals: bridging the gap between effects on individual behaviour and population level consequences. Oikos n/a.
Murphy, K.J., Ciuti, S., Kane, A., 2020. An introduction to agent-based models as an accessible surrogate to field-based research and teaching. Ecol. Evol. 10, 12482–12498.
Mysterud, A., Viljugrein, H., Rolandsen, C.M., Belsare, A.V., 2021. Harvest strategies for the elimination of low prevalence wildlife diseases. R. Soc. Open. Sci. 8, 210124.
Nielsen, S., Cranston, J., Stenhouse, G., 2009. Identification of priority areas for grizzly bear conservation and recovery in Alberta. Canada. J. Conser. Plann. 5, 38–60.
Nobert, B.R., 2012. Landscape ecology of mule deer (*Odocoileus hemionus*) and white-tailed deer (*O. virginianus*) with implications for chronic wasting disease. PhD Thesis.
Pays, O., Fortin, D., Gassani, J., Duchesne, J., 2012. Group dynamics and landscape features constrain the exploration of herds in fusion-fission societies: the case of European roe deer. PLoS. One 7, e34678.
Prieto, K., Ibarguen-Mondragon, E., 2019. Parameter estimation, sensitivity and control strategies analysis in the spread of influenza in Mexico. J. Phys.: Conf. Series 1408, 012020.
Raman, T.R.S., 1997. Factors influencing seasonal and monthly changes in the group size of chital or axis deer in southern India. J. Biosci. 22, 203–218.
Ramos-Fernández, G., Boyer, D., Gómez, V.P., 2006. A complex social structure with fission–fusion properties can emerge from a simple foraging model. Behav. Ecol. Sociobiol. (Print) 60, 536–549.
Ramsey, D.S.L., Efford, M.G., 2010. Management of bovine tuberculosis in brushtail possums in New Zealand: predictions from a spatially explicit, individual-based model: spatially explicit model of Tb in possums. J. Appl. Ecol. 47, 911–919.
Ramsey, D.S.L., O'Brien, D.J., Cosgrove, M.K., Rudolph, B.A., Locher, A.B., Schmitt, S.M., 2014. Forecasting eradication of bovine tuberculosis in Michigan white-tailed deer. J. Wildl. Manage. 78, 240–254.
Real, L.A., Biek, R., 2007. Spatial dynamics and genetics of infectious diseases on heterogeneous landscapes. J. Royal Soc. Interface 4, 935–948.
Riley, S.J., DeGloria, S.D., Elliot, R., 1999. A terrain ruggedness index that quantifies topographic heterogeneity. Intermountain J. Sci. 5, 23–27.
Salecker, J., Sciaini, M., Meyer, K., Wiegand, K., 2019. The nlrx r package: a next-generation framework for reproducible NetLogo model analyses. Methods Ecol. Evol. 00:2041–210X.
Schauber, E.M., Storm, D.J., Nielsen, C.K., 2007. Effects of joint space use and group membership on contact rates among white-tailed deer. J. Wildl. Manage. 71, 155–163.
Scherer, C., Radchuk, V., Franz, M., Thulke, H.-H., Lange, M., Grimm, V., Kramer-Schadt, S., 2020. Moving infections: individual movement decisions drive disease persistence in spatially structured landscapes. Oikos 129, 651–667.
Signer, J., Fieberg, J., Avgar, T., 2019. Animal movement tools (amt): r package for managing tracking data and conducting habitat selection analyses. Ecol. Evol. 9, 880–890.
Silbernagel, E.R., Skelton, N.K., Waldner, C.L., Bollinger, T.K., 2011. Interaction among deer in a chronic wasting disease endemic zone. J. Wildl. Manage. 75, 1453–1461.
Storm, D.J., Samuel, M.D., Rolley, R.E., Shelton, P., Keuler, N.S., Richards, B.J., Deelen, T.R.V., 2013. Deer density and disease prevalence influence transmission of chronic wasting disease in white-tailed deer. Ecosphere 4, art10.

Broeke ten, G., van Voorn, G., Ligtenberg, A., 2016. Which sensitivity analysis method should i use for my agent-based model? J. Artif. Societies Social Simulation 19, 5.
Thulke, H.H., Eisinger, D., 2008. The strength of 70%: revision of a standard threshold of rabies control. Dev. Biol. (Basel) 131, 291.
Thurfjell, H., Ciuti, S., Boyce, M.S., 2014. Applications of step-selection functions in ecology and conservation. Mov. Ecol. 2, 1–12.
Tosa, M.I., Schauber, E.M., Nielsen, C.K., 2015. Familiarity breed contempt: combining proximity loggers and GPS reveals female white-tailed deer (*Odocoileus virginianus*) avoiding close contact with neighbors. J. Wildl. Dis. 51, 79.
VerCauteren, K.C., Hygnstrom, S.E., 2004. White-tailed deer. Page in. editor. In: Wishart, D.J. (Ed.), Encyclopedia of the Great Plains. University of Nebraska Press.
von Neumann, J., 1951. Various Techniques Used in Connection With Random Digits. Pages 36–38. US Government Printing Office, Washington, DC.
Wells, K., Hamede, R.K., Jones, M.E., Hohenlohe, P.A., Storfer, A., McCallum, H.I., 2019. Individual and temporal variation in pathogen load predicts long-term impacts of an emerging infectious disease. Ecology 100, e02613.
White, L.A., Forester, J.D., Craft, M.E., 2017. Using contact networks to explore mechanisms of parasite transmission in wildlife. Biol. Rev. 92, 389–409.
White, L.A., Forester, J.D., Craft, M.E., 2018a. Dynamic, spatial models of parasite transmission in wildlife: their structure, applications and remaining challenges. J. Animal Ecol. 87, 559–580.
White, L.A., Forester, J.D., Craft, M.E., 2018b. Disease outbreak thresholds emerge from interactions between movement behavior, landscape structure, and epidemiology. Proc. National Acad. Sci. 115, 7374–7379.
Wilensky, U., 1999. Netlogo. Center for Connected Learning and Computer-Based Modeling. Northwestern University, Evanston, IL.